JOURNAL OF NATURAL PRODUCTS

Article

pubs.acs.org/jnp

Polycyclic Polyprenylated Acylphloroglucinol Congeners Possessing Diverse Structures from *Hypericum henryi*

Xing-Wei Yang,[†,⊥,∥] Ming-Ming Li,[†,∥] Xia Liu,[†,⊥] Daneel Ferreira,[‡] Yuanqing Ding,[§] Jing-Jing Zhang,[†,⊥] Yang Liao,[†,⊥] Hong-Bo Qin,*[,†] and Gang Xu*[,†]

[†]State Key Laboratory of Phytochemistry and Plant Resources in West China, Kunming Institute of Botany, Chinese Academy of Sciences, Kunming 650201, People's Republic of China

[‡]Department of Biomolecular Sciences, Division of Pharmacognosy, and [§]National Center for Natural Products Research, Research Institute of Pharmaceutical Science, School of Pharmacy, University of Mississippi, University, Mississippi 38677, United States

[⊥]University of Chinese Academy of Sciences, Beijing 100049, People's Republic of China

Supporting Information

ABSTRACT: Polycyclic polyprenylated acylphloroglucinols (PPAPs) are a class of hybrid natural products sharing the mevalonate/methylerythritol phosphate and polyketide biosynthetic pathways and showing considerable structural and bioactive diversity. In a systematic phytochemical investigation of *Hypericum henryi*, 40 PPAP-type derivatives, including the new compounds hyphenrones G−Q, were obtained. These compounds represent 12 different structural types, including four unusual skeletons exemplified by **5**, **8**, **10**, and **17**. The 12 different core structures found are explicable in terms of their biosynthetic origin. The structure of a known PPAP, perforatumone, was revised to hyphenrone A (**5**) by NMR spectroscopic and biomimetic synthesis methods. Several compounds exhibited inhibitory activities against acetylcholinesterase and human tumor cell lines. This study deals with the structural diversity, function, and biogenesis of natural PPAPs.

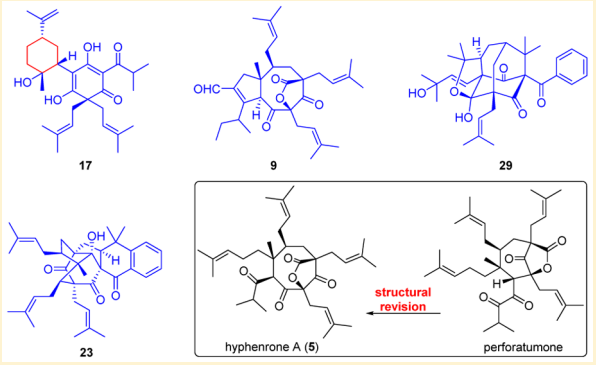

Polycyclic polyprenylated acylphloroglucinols (PPAPs), which possess highly oxygenated and various acylphloroglucinol-derived core structures decorated with prenyl substituents, are a group of structurally fascinating and synthetically challenging natural products that collectively exhibit a broad range of biological activities, such as tumor inhibitory, antimicrobial, anti-HIV, antioxidant, and antidepressant activities.[1,2] Biogenetically, PPAPs are derived from a "mixed" mevalonate/methylerythritol phosphate and polyketide biosynthetic pathway. Their acylphloroglucinol core structure is produced by a characteristic polyketide-type biosynthesis involving the condensation of one acyl-CoA and three malonyl-CoA units.[1,3] Prenylation of this core moiety affords monocyclic polyprenylated acylphloroglucinols (MPAPs), which may be further cyclized to PPAP-type metabolites with diverse carbon skeletons.[1,3]

Approximately 300 members of the PPAP family have been reported, of which the majority are bicyclic polyprenylated acylphloroglucinols (BPAPs) with a bicyclo[3.3.1]nonane-2,4,9-trione core, as exemplified by hyperforin and adhyperforin.[1,4] The adamantane-type PPAPs with "diamond-like" caged cores consist of about 70 members, with the first member, plukenetione A, being isolated in 1996.[5] Notably, the reported natural PPAPs have all been characterized from plants of the family Clusiaceae, and nearly half were isolated from the genus *Hypericum*.[1] Distributed in temperate regions throughout the world, *Hypericum* species have been used in traditional medicines in many countries.[6] The best known PPAP-type molecule is hyperforin (**1**), which exhibits cognitive-enhancing and memory-facilitating properties as well as potential neuroprotective effects against Alzheimer's disease.[7] In recent years, the fascinating chemical structures and intriguing biological activities of PPAPs have attracted widespread attention in terms of organic synthesis, phytochemistry, and biological evaluation.[1,2]

As part of a systematic search for new and bioactive natural PPAPs from plants in the genus *Hypericum*,[8] 40 PPAPs were characterized from *Hypericum henryi* H. Lév & Vaniot (Clusiaceae), a traditional Chinese medicinal plant used for the treatment of hepatitis and "dampness-heat" disease.[9] Previous phytochemical investigations on this species have led to the characterization of several xanthones and PPAPs, including four PPAP-type derivatives (hyphenrones A−D) possessing three unusual skeletons.[8c,10] The compounds obtained in the present study, including the new hyphenrones G−Q (**4**, **7**, **9**, **17**, **18**, **23**, **29**, **30**, and **32**−**34**), are comprised of

Received: January 21, 2015
Published: April 14, 2015

DOI: 10.1021/acs.jnatprod.5b00057
J. Nat. Prod. 2015, 78, 885−895

Scheme 1. Proposed Biosynthetic Pathways to the PPAPs from *H. henryi*: From Polyketides to Acylphloroglucinols, to Diverse PPAP-Type Derivatives (groups I–III)[a]

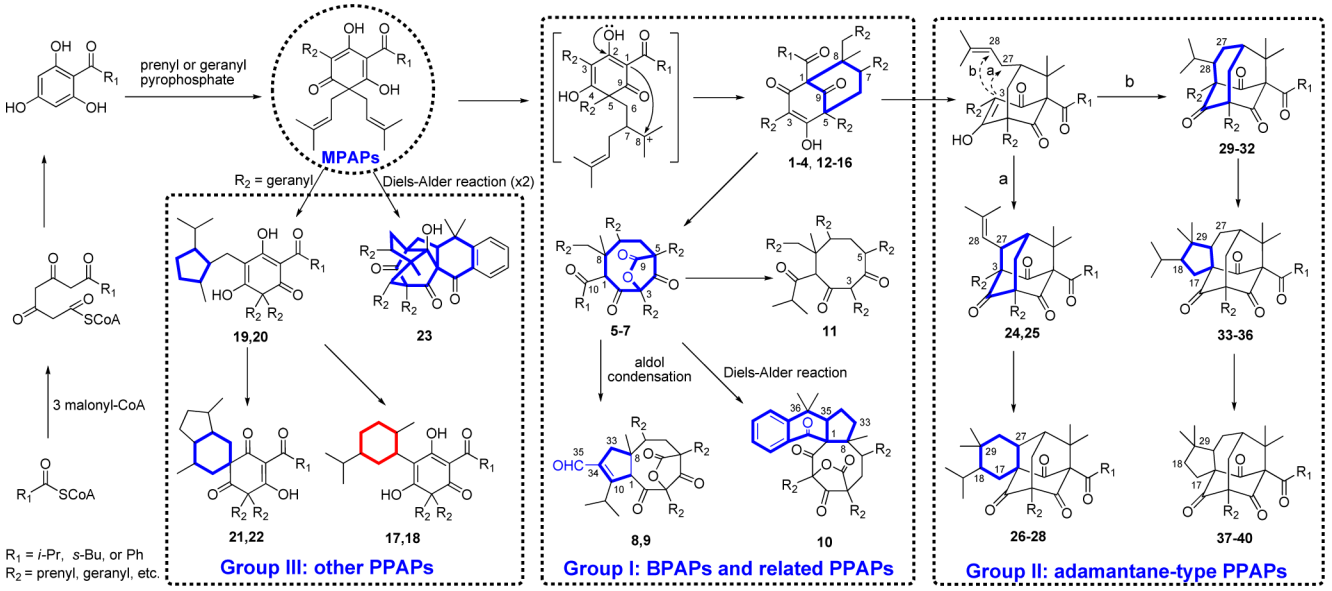

[a]Key: blue, newly formed rings in known skeletons; red, newly formed ring in novel skeleton.

Scheme 2. Biogenetic Pathways to BPAPs in Group I, Including the Oxidation, Ring Cleavage, and Cycloaddition of BPAPs into Three Unusual Carbon Skeletons Exemplified by 5, 8, and 10

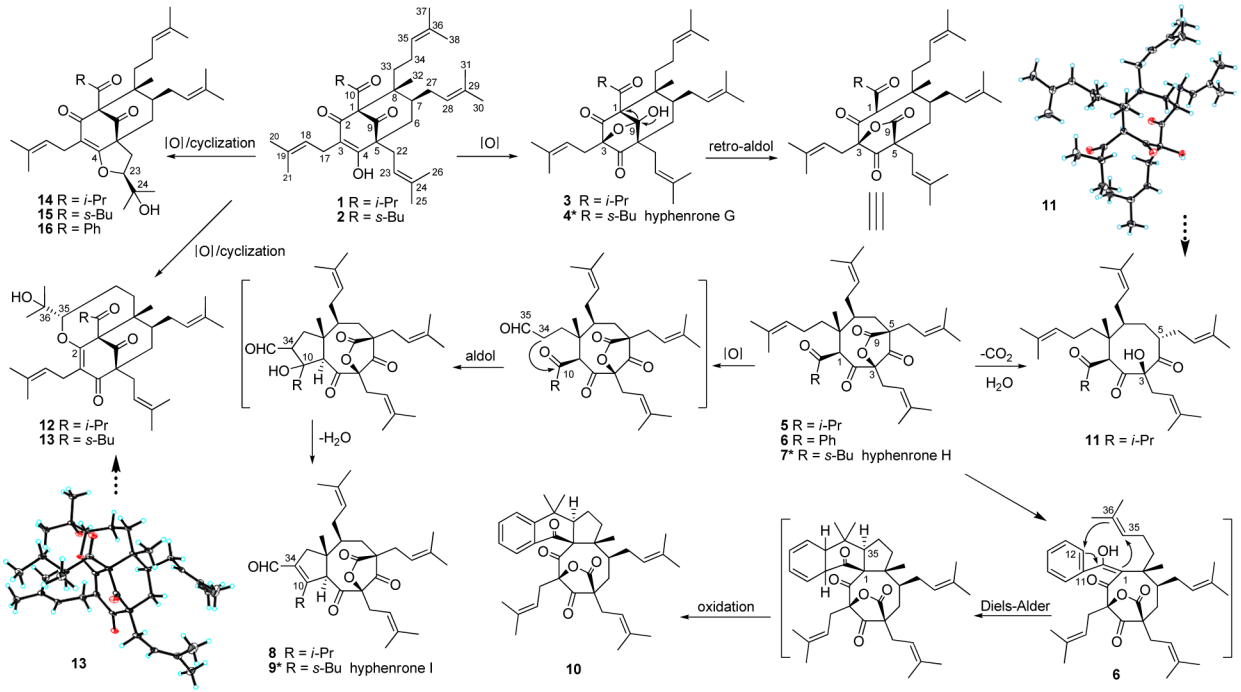

12 different structural types including four unusual skeletons as exemplified by **5**, **8**, **10**, and **17**. Their structures were determined by spectroscopic methods and single-crystal X-ray diffraction analysis. By combining NMR comparison and biomimetic synthesis verification, the structure of perforatumone,[11] a known PPAP with a seven-membered carbon skeleton, was shown to be identical to hyphenrone A, possessing an eight-membered carbocyclic core, reported by our group previously.[8c] Interestingly, these 12 diverse carbon skeletons are presumably all derived from a common biosynthetic pathway via different cyclizations of the less complex MPAPs. Characterization of intermediate compounds, present in trace amounts, has indicated that these PPAP profiles are generated via three major biosynthetic pathways and may be divided into three groups (I–III) according to their different scaffolds.

RESULTS AND DISCUSSION

The MeOH extract of *H. henryi* was subjected to purification using silica gel column and preparative thin-layer chromatog-

DOI: 10.1021/acs.jnatprod.5b00057
J. Nat. Prod. 2015, 78, 885–895

Table 1. ^{13}C (150 MHz) and ^{1}H (600 MHz) NMR Spectroscopic Data of 4, 5, 7, and 9

	4[a]		5[a]		7[b]		9[c]	
no.	δ_C, type	δ_H mult. (J in Hz)	δ_C, type	δ_H mult. (J in Hz)	δ_C, type	δ_H mult. (J in Hz)	δ_C, type	δ_H mult. (J in Hz)
1	71.4, C		62.5, CH	4.47 s	63.6, CH	4.50 s	67.5, CH	4.28 d (2.6)
2	207.1, C		196.9, C		198.1, C		201.5, C	
3	97.2, C		95.5, C		95.7, C		96.0, C	
4	209.4, C		206.3, C		206.8, C		208.8, C	
5	54.9, C		56.7, C		57.3, C		56.6, C	
6	33.0, CH_2	1.86 m	36.5, CH_2	1.57 overlap	37.2, CH_2	β 1.62 overlap	39.0, CH_2	β 1.80 dd (15.8, 7.5)
		1.25 overlap				α 1.58 overlap		α 1.75 overlap
7	41.8, CH	1.02 m	39.9, CH	1.57 overlap	40.7, CH	1.56 m	45.0, CH	1.71 m
8	47.0, C		48.4, C		48.7, C		55.1, C	
9	108.5, C		171.9, C		172.0, C		174.2, C	
10	218.0, C		206.3, C		205.9, C		166.8, C	
11	46.6, CH	2.95 m	42.4, CH	2.61 sept (6.8)	49.6, CH	2.48 m	37.6, CH	2.60 m
12	16.5, CH_3	0.90 d (6.8)	18.9, CH_3	1.07 d (6.8)	16.0, CH_3	0.98 d (6.8)	20.7, CH_3	1.25 d (7.2)
13	25.3, CH_2	1.58 overlap	18.8, CH_3	1.04 d (6.8)	26.7, CH_2	1.65 overlap	31.9, CH_2	1.64 m
						1.29 m		
14	11.8, CH_3	0.87 t (7.8)			11.5, CH_3	0.90 t (7.5)	13.2, CH_3	0.94 t (7.4)
17	24.0, CH_2	2.46 dd (15.0, 7.0)	29.7, CH_2	2.86 dd (15.0, 7.0)	30.4, CH_2	2.96 dd (15.0, 7.0)	32.1, CH_2	2.86 dd (15.0, 7.8)
		2.58 dd (15.0, 7.0)		2.57 dd (15.0, 7.0)		2.60 dd (15.0, 7.0)		2.54 overlap
18	116.2, CH	5.01 t (7.0)	113.5, CH	4.95 t (7.0)	114.9, CH	4.93 t (7.0)	115.1, CH	4.90 t (7.8)
19	136.0, C		138.8, C		138.9, C		140.2, C	
20	26.1, CH_3	1.63 s	25.8, CH_3	1.65 s	25.9, CH_3	1.65 s	26.4, CH_3	1.66 s
21	18.2, CH_3	1.60 s	18.2, CH_3	1.65 s	18.1, CH_3	1.65 s	18.3, CH_3	1.66 s
22	31.2, CH_2	2.39 m	27.5, CH_2	2.52 dd (15.0, 7.0)	28.2, CH_2	2.55 dd (15.0, 7.5)	30.4, CH_2	2.50 dd (14.3, 7.2)
				2.12 dd (15.0, 7.0)		2.10 dd (15.0, 7.5)		2.20 dd (14.3, 7.2)
23	119.1, CH	5.26 t (7.0)	117.5, CH	4.71 t (7.0)	118.7, CH	4.72 t (7.5)	118.8, CH	4.73 t (7.2)
24	134.0, C		136.3, C		136.3, C		137.4, C	
25	26.3, CH_3	1.71 s	25.8, CH_3	1.61 s	25.8, CH_3	1.53 s	26.3, CH_3	1.62 s
26	17.9, CH_3	1.54 s	18.1, CH_3	1.68 s	18.2, CH_3	1.66 s	18.2, CH_3	1.66 s
27	28.7, CH_2	2.09 m	28.8, CH_2	2.00 overlap	29.2, CH_2	2.04 overlap	31.5, CH_2	2.02 brd (14.3)
				1.74 m		1.88 m		1.86 m
28	122.2, CH	4.91 t (7.0)	122.8, CH	4.90 t (7.0)	123.7, CH	5.14 m	123.7, CH	5.12 m
29	133.7, C		134.8, C		135.1, C		135.9, C	
30	26.0, CH_3	1.68 s	26.0, CH_3	1.75 s	26.1, CH_3	1.77 s	26.1, CH_3	1.77 s
31	18.1, CH_3	1.54 s	18.0, CH_3	1.59 s	18.1, CH_3	1.64 s	18.1, CH_3	1.64 s
32	15.7, CH_3	1.00 s	17.8, CH_3	1.08 s	16.3, CH_3	1.09 s	15.5, CH_3	0.80 s
33	37.1, CH_2	1.75 overlap	38.6, CH_2	1.46 m	38.9, CH_2	1.53 m	44.8, CH_2	β 2.54 overlap
		1.59 overlap		1.31 m		1.40 m		α 2.35 dd (14.7, 2.6)
34	24.0, CH_2	2.25 m	21.6, CH_2	1.96 m	22.3, CH_2	2.01 m	141.0, C	
		1.85 m		1.87 m		1.92 m		
35	124.3, CH	4.96 t (7.0)	122.5, CH	4.99 (brd, 7.0)	123.9, CH	4.97 t (6.6)	190.0, C	10.09 s
36	131.9, C		132.4, C		132.6, C			
37	26.1, CH_3	1.65 s	25.7, CH_3	1.66 (s)	25.9, CH_3	1.65 s		
38	17.9, CH_3	1.58 s	18.0, CH_3	1.63 (s)	17.9, CH_3	1.63 s		

[a]Recorded in $CDCl_3$. [b]Recorded in acetone-d_6. [c]Recorded in methanol-d_4.

raphy, coupled with RP-18 silica gel HPLC, and yielded a total of 40 compounds based on 12 different structural types. These diverse carbon skeletons were all derived from the less complex MPAPs by different cycloadditions, such as aldol condensations and Diels−Alder additions. Their structures were determined by spectroscopic methods coupled with single-crystal X-ray diffraction analysis of **11**, **13**, **19**, **26**, and **38**, representing five different carbon frameworks. According to their different scaffolding constructs, these 40 isolates could be divided into three groups (I−III) as shown in Scheme 1. The four core structures in group I, represented by **1**, **5**, **8**, and **10**, are BPAPs or related PPAPs, with **10** possessing a complex 6/6/5/8/5 pentacyclic system with six stereogenic centers derived from the normal BPAPs. The adamantane-type PPAPs, derived via linkage of C-3/C-27 or C-3/C-28 of normal *endo*-BPAPs, are included in group II and consist of four different scaffolds as exemplified by **24**, **26**, **29**, and **33**. The other four types, as illustrated by **17**, **19**, **21**, and **23**, were assigned to group III.

Group I is perhaps the most interesting of the three groups due to the structural novelty of constituents. In fact, the carbon frameworks of **5**, **8**, and **10** are all unusual skeletons derived from normal BPAPs possessing the bicyclo[3.3.1]nonane-2,4,9-trione core. Biosynthetically, **5**−**7** are presumably formed by cleavage of the C-1/C-9 bond of hemiketal derivatives such as **3** via a retro-aldol mechanism and subsequent formation of a five-membered lactone moiety. The structures of **8** and **9** possess unusual 5/8/5 fused ring systems and may be derived from **5** and **7**, respectively, via oxidative cleavage of the C-35/C-36

DOI: 10.1021/acs.jnatprod.5b00057
J. Nat. Prod. 2015, 78, 885−895

double bond followed by formation of the cyclopentene moiety by aldol condensation. The structure of **10**, featuring a pentacyclic 6/6/5/8/5 fused ring system, is presumably formed via an intermolecular Diels–Alder cycloaddition of **6** as a key step (Scheme 2).

Hyphenrone G (**4**) was obtained as a colorless gum. Its molecular formula was established by its ^{13}C NMR and HRTOFMS data (*m*/*z* 589.3871, $[M + Na]^+$) as $C_{36}H_{54}O_5$, 14 mass units more than that of 3-hydroxyhyperforin-3,9-hemiketal (**3**).[12] Comparison of the ^1H and ^{13}C NMR spectroscopic data of **4** (Table 1) with those of **3** indicated that the isopropyl group in **3** should be replaced by a *sec*-butyl group (C-11, δ_C 46.6; C-12, δ_C 16.5; C-13, δ_C 25.3; and C-14, δ_C 11.8) in **4**. The correlations of Me-14 (δ_H 0.87) with C-11 and C-13 and of Me-12 (δ_H 0.90) with C-11 and C-10 (δ_C 218.0) in the HMBC spectrum were indicative of such a difference (Figure 1). Other

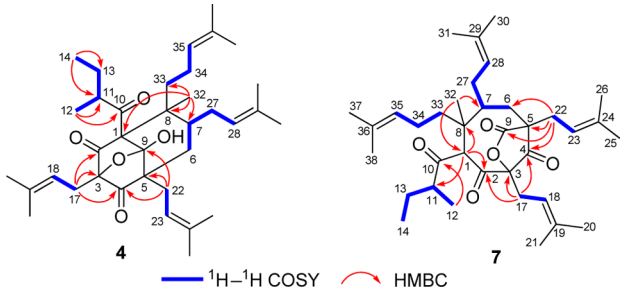

Figure 1. Key HMBC and ^1H–^1H COSY correlations of **4** and **7**.

parts of **4** were identical to those of **3** by analysis of the 2D NMR spectroscopic data. Similarly, hyphenrones H (**7**) and I (**9**) shared the same carbon skeletons and relative configurations of hyphenrones A (**5**) and C (**8**),[8c] respectively, by analysis of their HREIMS and NMR data (Table 1). The structural novelty of **7** (Figure 1) and **9** is hence attributable to the presence of a *sec*-butyl group at C-10, instead of the isopropyl group in **5** and **8**.

In addition, perforatumone, isolated from *H. perforatum* in 2004, was reported to possess a novel PPAP skeleton with a seven-membered carbon core.[11a] The reported ^1H and ^{13}C NMR spectroscopic data of this compound are identical to those of **5** (Table 1), indicating that one of the two structures must have been assigned incorrectly. The deshielded C-1 (δ_C 62.5) and H-1 (δ_H 4.47, s) resonances indicate that this methine functionality is more likely adjacent to two carbonyl groups (C-2 and C-10) in **5**, rather than one carbonyl group in perforatumone, hence supporting the structural assignment of **5**.[8c] In order to clarify the structure of these two compounds, a biomimetic synthesis of hyphenrone F (**11**) from **3** via compound **5** was performed as shown in Scheme 3. A piperidine-induced retro-aldol reaction of **3** afforded **5** in 40% yield. When subjected to reaction with triethylamine in MeOH at 50 °C, **5** was converted into **11** via hydrolysis and subsequent decarboxylation of the intermediate β-keto carboxylic acid. Single-crystal X-ray diffraction analysis of **11** confirmed its structure unequivocally and indicated that the structure of perforatumone is indeed identical to that of hyphenrone A (**5**).

Definition of the absolute configurations of PPAPs is challenging because they are usually isolated as gums or oils. However, crystals of **11** (CCDC 962625) and **13** (CCDC 962624) suitable for X-ray diffraction analysis were obtained

Scheme 3. Structural Revision of Perforatumone and the Biomimetic Transformation of 3 via 5 into 11

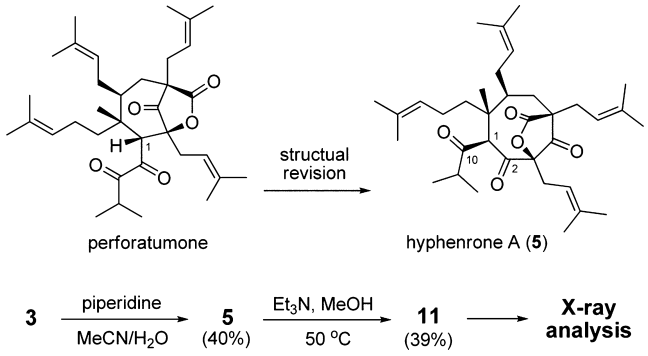

from MeOH. The X-ray data indicated that the absolute configurations of C-1, C-3, C-5, C-7, and C-8 in **11** and **13** were consistent with those of hyperforin (**1**) and **10** established previously.[1,8c] In addition, the 16 PPAPs in group I are closely related biosynthetically (Scheme 2). Compounds **1** and **2** should be the precursors of the 2,35-etherocyclic derivatives **12** and **13**,[12] the 4,23-etherocyclic derivatives **14**–**16**,[10c,13] and the hemiketal derivatives **3** and **4**. Compounds **5**–**7** are derived from **3** and **4** and yielded **8**–**11** via the transformations shown in Scheme 2. Thus, the absolute configuration of these PPAPs should be consistent with one another.

The adamantane-type PPAPs with "diamond-like" caged cores were assigned to group II. Historically, adamantane-type compounds have attracted much interest from medicinal chemists since the early 1960s, when amantadine was introduced to the clinic for the treatment of influenza.[14] In fact, the adamantyl structural moiety is present in a number of compounds in current clinical use and in many more compounds that are in development as potential agents for the treatment of iron overload disease, cancer, malaria, and tuberculosis.[15] From a medicinal chemistry perspective, the adamantyl group can be used either as a scaffold for the development of therapeutic agents, e.g., memantine and amantadine, or as a modifier of the pharmacokinetics of a compound.[14,15] Group II comprises 17 adamantane-type PPAPs (**24**–**40**) including the five new hyphenrones M–Q (**29**, **30**, **32**–**34**) shown in Scheme 4. Thus far, about 70 natural adamantane-type PPAPs based on four different carbon skeletons have been reported. They may be divided into adamantine tricyclo[3.3.1.1]decane (**24**–**28**) and *homo*-adamantane tricyclo[4.3.1.1]undecane (**29**–**40**) types.[2h,5,16] Both types are derived biosynthetically from the *endo*-BPAPs with the bicyclo[3.3.1]nonane core via the strongly nucleophilic enolic C-3 cyclizing onto C-27 and C-28, respectively. Two secondary skeletons exemplified by **26** and **33** are derived from C-18/C-29 cyclization in the adamantane- and *homo*-adamantane-type PPAPs, respectively (Scheme 4).[5,16]

Hyphenrone M (**29**) was assigned the molecular formula $C_{33}H_{42}O_6$ from its ^{13}C NMR and HREIMS data. The ^1H and ^{13}C NMR spectroscopic data of **29** (Tables 2 and 3) resembled those of sampsonione A, a *homo*-adamantane-type PPAP.[16a] Instead of the olefinic quaternary carbon at δ_C 133.0 (C-19) and a methylene (δ_C 33.7, C-17) in sampsonione A, an oxygenated tertiary carbon at δ_C 71.9 and an olefinic methine (δ_C 126.4) appeared in **29**, assuming hydroxylation of C-19 and formation of a $\Delta^{17,18}$ double bond. This assumption was supported by the correlations of H-17 (δ_H 6.45, J = 16.2 Hz)

DOI: 10.1021/acs.jnatprod.5b00057
J. Nat. Prod. 2015, 78, 885–895

Scheme 4. Proposed Biosynthetic Pathway of Group II PPAPs: Cyclization of *endo*-BPAPs Generating Adamantane- and *homo*-Adamantane-Type PPAPs

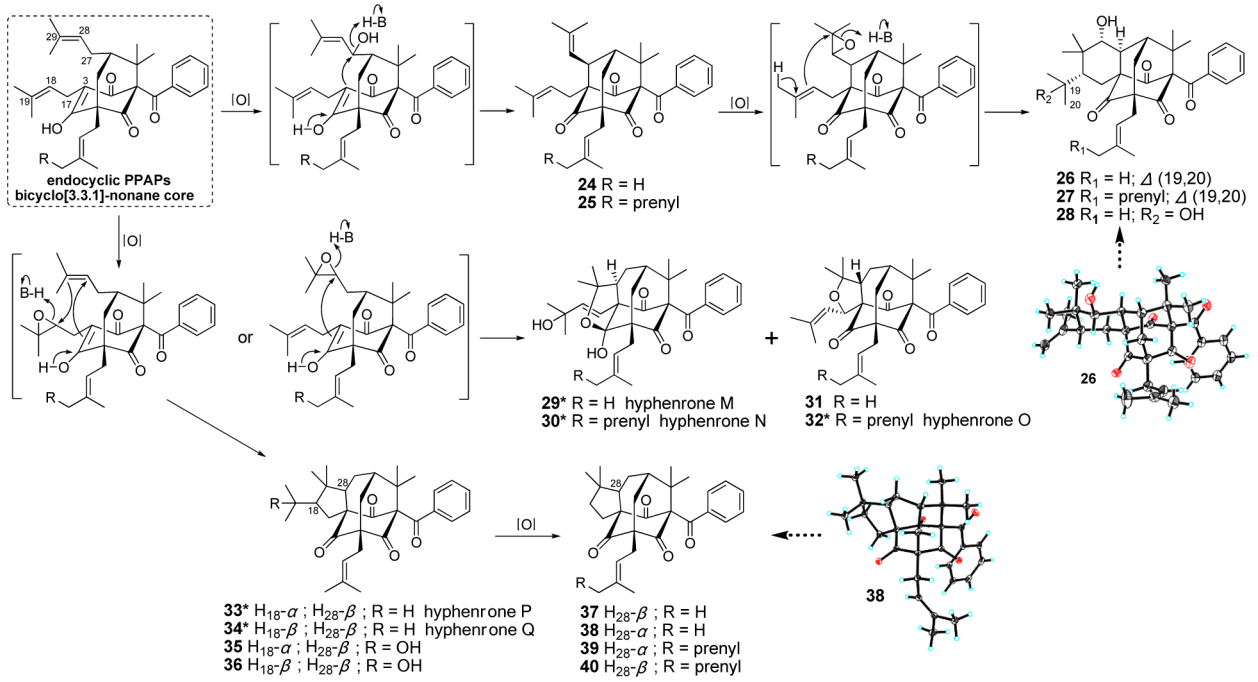

with C-2 (δ_C 204.9), C-3, (δ_C 68.9), and C-4 (δ_C 110.5) and of both Me-20 (δ_H 1.19) and Me-20 (δ_H 1.16) with C-18 (δ_C 143.3) and C-19 in the HMBC spectrum (Figure 2). Likewise, the structure of hyphenrone N (**30**) was shown to be a homologue of **29**, with the C-5 prenyl group in the latter being replaced by a geranyl group in **30** (Tables 2 and 3). The 2D NMR data showed that other structural units of **29** and **30** are the same as those of sampsonione A.

The molecular formula of hyphenrone O (**32**) was determined as $C_{38}H_{48}O_5$ by analysis of its ^{13}C NMR (Table 2) and HRESIMS (*m*/*z* 539.2767, $[M + Na]^+$) data. The $^1H-^1H$ COSY and HMBC spectroscopic data (Figure 2) suggested that **32** has the same carbon scaffold as hypersampsone O (**31**)[16g] and that it carries a C-5 geranyl side chain. In the ROESY spectrum, the correlations of Me-33 (δ_H 1.42) with H-27α (δ_H 2.22), of H-27α with Me-31 (δ_H 1.12), and of Me-30 (δ_H 1.30) with H-17 (δ_H 5.54) and H-28 (δ_H 2.69), coupled with the rigid caged skeleton, defined the relative configurations of **32**.

On the basis of analysis of its MS and 1D and 2D NMR data (Tables 2 and 3), hyphenrone P (**33**) was shown to possess the same backbone and relative configuration as hypersampsone E.[17] The structural novelty of **33** involves the presence of a C-5 prenyl rather than a geranyl group. Hyphenrone Q (**34**) is the C-18 epimer of **33**, as exemplified by the NOE association from H-6 (δ_H 2.47) to H-28 (δ_H 2.10) and from Me-30 (δ_H 1.02) to H-28 and H-18 (δ_H 1.45) in the ROESY spectrum of **34** (Tables 2 and 3).

The four different caged core structures in group II are all derived from a common biosynthetic pathway. Therefore, it is reasonable to assume that the absolute configurations of these caged PPAPs are similar. This was confirmed by refinement of the Cu Kα data of the crystals of **26** [CCDC 962622, the Hooft parameter is 0.10(6) for 2577 Bijvoet pairs] and **38** [CCDC 962623, the Flack parameter is 0.01(13)],[18] indicating (1*R*,3*R*,5*R*,7*R*,27*S*) and (1*R*,3*R*,5*R*,7*S*,28*R*) absolute configurations for the adamantane- and *homo*-adamantane-type PPAPs, respectively.

The seven members (**17**−**23**) in the miscellaneous group III are derived from direct cyclizations of PPAPs rather than via formation of the BPAPs (Scheme 5) and are constructed from four core structures as exemplified by **17**, **19**, **21**, and **23**. Hyphenrones J (**17**) and K (**18**), featuring an unprecedented six-membered ring connected to the phloroglucinol core, presumably are derived biosynthetically from **19** (CCDC 963510) via rearrangements involving the formation and cleavage of a cyclopropane intermediate. Compounds **21** and **22**, featuring an octahydrospiro[cyclohexan-1,5′-indene] core, are considered to be the intramolecular cyclization products of **19**.[19] Hyphenrone L (**23**), with a hexacyclic core, representing the most complex PPAP, is likely derived from a pentaprenylated MPAP via successive intramolecular [2 + 4] cycloadditions.[20]

Hyphenrone J (**17**) was obtained as a light yellow gum, exhibited an ion peak at *m*/*z* 507.3093 $[M + Na]^+$ in its HRESIMS, and was assigned a molecular formula of $C_{30}H_{44}O_5$, the same as hypercalin C (**19**).[19a] Analysis of the 1D and 2D NMR data (Table 4) revealed that **17** is a derivative of an MPAP and shares the same acylphloroglucinol core as **19**. However, a difference was found in the C-3 side chain from the observed long-range correlations in the HMBC spectrum from the C-7 methine proton at δ_H 3.28 to three carbons (C-2, δ_C 191.1; C-3, δ_C 112.6; and C-4, δ_C 177.9) of the acylphloroglucinol core, suggesting that the C-7 methine was linked to C-3 in **17** rather than a methylene in **19** (Figure 3). In addition to the HMBC correlations of Me-10 (δ_H 1.23) to C-7, C-9, and C-11, the $^1H-^1H$ COSY correlations of H-7/H-8/H-13/H-12/H-11 led to the arbitrary assignment of the six-membered carbocyclic in **17**. The strong ROESY correlations of Me-10/H-7 and H-7/H-13 established the cofacial orientations for H-7, H-13, and Me-10. Therefore, the structure of **17** was elucidated as possessing an unprecedented six-membered carbocyclic ring

DOI: 10.1021/acs.jnatprod.5b00057
J. Nat. Prod. 2015, 78, 885−895

Table 2. ^{13}C (150 MHz, δ in ppm) NMR Spectroscopic Data of 29, 30, and 32−34

no.	29[a]	30[b]	32[b]	33[b]	34[b]
1	82.2, C	81.4, C	83.0, C	82.6, C	82.0, C
2	204.9, C	203.8, C	200.2, C	205.7, C	204.5, C
3	68.9, C	68.2, C	77.5, C	73.0, C	72.4, C
4	110.5, C	110.3, C	203.4, C	204.1, C	203.5, C
5	60.9, C	60.1, C	69.0, C	68.5, C	68.4, C
6	33.0, CH_2	32.5, CH_2	36.1, CH_2	35.5, CH_2	35.6, CH_2
7	44.7, CH	44.1, CH	42.8, CH	42.9, CH	42.7, CH
8	48.8, C	48.1, C	48.7, C	48.0, C	48.4, C
9	211.5, C	210.1, C	205.0, C	206.2, C	206.0, C
10	196.1, C	195.3, C	193.7, C	193.8, C	193.7, C
11	134.7, C	136.6, C	135.8, C	135.9, C	135.9, C
12,16	130.5, CH	130.1, CH	129.6, CH	129.2, CH	129.2, CH
13,15	129.0, CH	128.6, CH	129.1, CH	129.1, CH	129.1, CH
14	133.0, CH	132.6, CH	132.9, CH	133.2, CH	133.1, CH
17	126.4, CH	125.0, CH	75.3, CH	34.5, CH_2	33.9, CH_2
18	143.3, CH	143.8, CH	121.3, CH	57.0, CH	58.0, CH
19	71.9, C	70.9, C	139.1, C	29.6, CH	29.6, CH
20	29.2, CH_3	30.0, CH_3	26.8, CH_3	23.8, CH_3	23.3, CH_3
21	29.6, CH_3	29.8, CH_3	18.5, CH_3	22.5, CH_3	23.0, CH_3
22	28.9, CH_2	28.6, CH_2	29.5, CH_2	29.9, CH_2	30.3, CH_2
23	122.3, CH	122.0, CH	120.1, CH	120.1, CH	120.1, CH
24	137.2, C	137.7, C	139.1, C	135.3, C	135.3, C
25	26.3, CH_3	40.7, CH_2	40.7, CH_2	26.2, CH_3	26.2, CH_3
26	18.0, CH_3	16.2, CH_3	16.4, CH_3	18.0, CH_3	18.0, CH_3
27	26.7, CH_2	26.3, CH_2	25.8, CH_2	26.3, CH_2	23.5, CH_2
28	53.4, CH	52.9, CH	54.8, CH	56.1, CH	56.5, CH
29	85.3, C	84.7, C	82.7, C	45.2, C	46.8, C
30	27.4, CH_3	27.4, CH_3	30.7, CH_3	27.0, CH_3	28.8, CH_3
31	34.0, CH_3	33.7, CH_3	25.1, CH_3	26.7, CH_3	15.9, CH_3
32	25.2, CH_3	25.1, CH_3	25.6, CH_3	25.2, CH_3	25.4, CH_3
33	22.4, CH_3	22.3, CH_3	22.9, CH_3	22.6, CH_3	22.6, CH_3
34		27.3, CH_2	27.2, CH_2		
35		125.1, CH	125.0, CH		
36		131.7, C	131.8, C		
37		25.9, CH_3	25.9, CH_3		
38		17.7, CH_3	17.7, CH_3		

[a]Recorded in methanol-d_4. [b]Recorded in acetone-d_6.

connected to the phloroglucinol core. Biosynthetically, **17** seems to be derived from the same precursor as **19**. However, it more likely originates from **19** via a rearrangement involving the formation and cleavage of a cyclopropane intermediate, since the carbon skeleton of the C_{10} unit connected to C-3 is not consistent with the isoprene rule (Scheme 5). Hyphenrone K (**18**) was shown to be an analogue of **17** by replacement of the isopropyl moiety in **17** with a *sec*-butyl group in **18** from the MS and NMR data obtained (Table 4).

The molecular formula of hyphenrone L (**23**) was determined to be $C_{38}H_{48}O_4$ from its ^{13}C NMR and HREIMS (m/z 591.3444, $[M + Na]^+$) data, 68 mass units more than that of garcibracteatone.[20] Comparison of the NMR spectroscopic data (Table 5) of **23** with those of garcibracteatone indicated an extra prenyl group (δ_C 27.8, C-34; 126.9, C-35; 132.3, C-36; 26.0, C-37; and 18.4, C-38) to be present and linked to the C-27 methine δ_C 54.8 (C-27). The correlations of H-27 (δ_H 1.76)/H-34 (δ_H 2.17 and 1.60)/H-35 (δ_H 4.90) in the $^1H-^1H$ COSY spectrum, as well as the correlations from Me-28 (δ_H 1.43) to C-27 and C-26 (δ_C 46.8) in the HMBC spectrum, confirmed such a difference (Figure 3). The relative configuration of the C-27 stereogenic center in **23** was indicated by the NOE correlation between Me-28 and H-34 (δ_H 2.17) in the ROESY spectrum.

Considering the fact that several cytotoxic PPAPs have been isolated previously[8] and that these types of metabolites are associated with neurodegenerative diseases, such as Alzheimer's disease,[7] the inhibitory activities of the aforementioned compounds were examined against acetylcholinesterase (AChE) and the five human tumor cell lines HL-60, A-549, SMMC-7721, MCF-7, and SW-480 (Table 6). Compounds **17** and **19** exhibited cytotoxic activities (IC_{50} 1.7−8.9 μM) against the cancer cell lines using the MTT method.[21] In the AChE inhibition assay using the Ellman method,[22] compounds **13**, **17**, **26**, and **40** exhibited AChE inhibitory activities (IC_{50} 37.2, 25.4, 26.4, and 9.8 μM, respectively). Notably, the PPAPs that possess a lactone moiety (**5** and **7**−**10**) exhibited significant negative inhibitory activities (approximately −100% for each) at 50 μM.

PPAPs are a class of promising molecules for drug development, especially the BPAPs and adamantane-type PPAPs. The presence of multiple prenyl groups and the derived complex ring systems in the structures of PPAPs are rare among plant secondary metabolites. Generally, polyketide

DOI: 10.1021/acs.jnatprod.5b00057
J. Nat. Prod. 2015, 78, 885−895

Table 3. ^{1}H (600 MHz, δ in ppm) NMR Spectroscopic Data of 29, 30, and 32−34

no.	29[a]	30[b]	32[b]	33[b]	34[b]
6	a 2.33 dd (15.0, 6.4)	a 2.36 dd (15.4, 6.4)	a 2.58 dd (15.0, 7.5)	a 2.49 overlap	a 2.49 overlap
	b 2.21 brd (15.0)	b 2.24 brd (15.4)	b 2.36 brd (15.0)	b 2.40 brd (14.7)	b 2.47 brd (15.0)
7	1.76 brt (7.5)	1.83 brt (6.4)	2.24 brt (7.5)	2.22 m	2.25 brt (7.9)
12, 16	7.40 d (8.0)	7.46 d (8.0)	7.08 d (8.0)	7.11 d (8.0)	7.04 d (8.0)
13, 15	7.29 t (8.0)	7.30 t (8.0)	7.31 t (8.0)	7.38 t (8.0)	7.38 t (8.0)
14	7.39 t (8.0)	7.42 t (8.0)	7.50 t (8.0)	7.49 t (8.0)	7.47 t (8.0)
17	6.45 d (16.2)	6.56 d (16.2)	5.54 d (9.4)	β 2.47 overlap	β 2.56 dd (12.8, 7.1)
				α 1.80 dd (13.2, 6.4)	α 2.05 m
18	5.99 d (16.2)	6.04 d (16.2)	4.98 d (9.4)	2.00 m	1.45 m
19				1.63 m	1.67 m
20	1.19 s	1.15 s	1.58 s	0.95 d (6.4)	1.00 d (6.4)
21	1.16 s	1.14 s	1.84 s	0.89 d (6.4)	0.94 d (6.4)
22	2.74 dd (14.6, 8.0)	2.78 dd (14.3, 7.8)	2.53 dd (15.4, 7.5)	2.56 dd (15.0, 7.5)	2.57 overlap
	2.43 dd (14.6, 8.0)	2.46 dd (14.3, 7.8)	2.49 dd (15.4, 7.5)	2.51 overlap	2.49 dd (15.0, 7.5)
23	5.39 brt (8.0)	5.39 brt (7.8)	5.27 brt (7.5)	5.26 brt (7.5)	5.29 brt (7.5)
25	1.71 s	2.08 m	2.02, m	1.69 s	1.69 s
		2.02 m			
26	1.65 s	1.63 s	1.65 s	1.65 s	1.65 s
27	2.07 dd (16.6, 8.5)	2.08 overlap	2.22 dd (15.4, 11.6)	2.02 m	1.93 m
	1.98 dd (16.6, 7.5)	1.98 dd (17.3, 7.6)	2.04 m	1.92 m	1.86 m
28	2.65 d (7.5)	2.68 d (7.6)	2.69 dd (11.7, 8.6)	2.20 m	2.10 m
30	1.43 s	1.44 s	1.30 s	0.97 s	1.02 s
31	1.51 s	1.50 s	1.12 s	0.99 s	0.83 s
32	1.34 s	1.37 s	1.36 s	1.36 s	1.38 s
33	1.16 s	1.18 s	1.42 s	1.35 s	1.35 s
34		2.08 overlap	2.06, m		
		2.02 overlap			
35		5.09 t (6.8)	5.07 t (7.0)		
37		1.63 s	1.64 s		
38		1.57 s	1.57 s		

[a]Recorded in methanol-d_4. [b]Recorded in acetone-d_6.

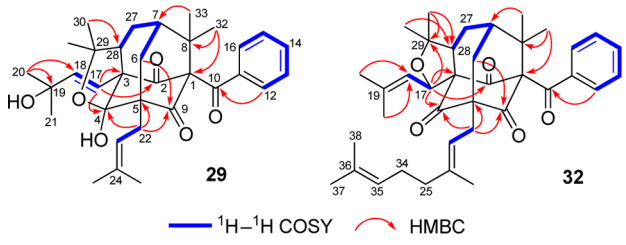

Figure 2. Key HMBC and ^{1}H−^{1}H COSY correlations of 29 and 32.

and prenylation synthases are widespread in plants and often coexist in certain species, as evidenced by the presence of natural prenylated flavones and xanthones.[23] Notably, the presence of the complex class of PPAP metabolites is hitherto restricted to plants in the Clusiaceae, which indicated the prenyltransferase in these plants should possess high activity and selectivity. Furthermore, the intriguing structures of these PPAPs and their biogenetic relationship also suggested there are complex postmodification processes including oxidation, rearrangement, and cyclization in plants. Although many studies about the biosynthesis of PPAPs have been reported,[3] more in-depth research works are still needed to uncover the interesting pathway of this special group of metabolites.

EXPERIMENTAL SECTION

General Experimental Procedures. Melting points were obtained on an X-4 micro melting point apparatus. Optical rotations were measured on a JASCO P-1020 polarimeter. UV spectra were recorded on a Shmadzu UV-2401PC spectrometer. IR spectra were recorded on a Bruker FT-IR Tensor-27 infrared spectrophotometer with KBr disks. 1D and 2D NMR spectra were recorded on a Bruker DRX-600 spectrometer using TMS as an internal standard. Unless otherwise specified, chemical shifts (δ) are expressed in ppm with reference to the solvent signals. ESIMS and HREIMS data were acquired on Waters Xevo TQS and Waters AutoSpec Premier P776 mass spectrometers, respectively. X-ray data were generated using a Bruker Apex Duo instrument. Semipreparative HPLC was performed on an Agilent 1100 HPLC with a Zorbax SB-C_{18} (9.4 × 250 mm) column. Silica gel (100−200 and 200−300 mesh, Qingdao Marine Chemical Co., Ltd., Qingdao, People's Republic of China) and MCI gel (75−150 μm, Mitsubishi Chemical Corporation, Tokyo, Japan) were used for column chromatography. Fractions were monitored by TLC (GF 254, Qingdao Marine Chemical Co., Ltd.), and spots were visualized by heating silica gel plates immersed in H_2SO_4 in ethanol.

Plant Material. The aerial parts of *H. henryi* were collected at Hongtudi in Dongchuan Prefecture, Yunnan Province, People's Republic of China, in April 2011. The plant was identified by Dr. E. D. Liu, and a voucher specimen (201104H01) has been deposited at the Kunming Institute of Botany.

Extraction and Isolation. The aerial parts of *H. henryi* (18.0 kg) were powdered and percolated with MeOH (2 × 20 L) at room temperature for 24 h and filtered, and the solvent was evaporated in vacuo. The crude extract (1.8 kg) was subjected to silica gel column chromatography eluted with $CHCl_3$ to afford a PPAP-rich fraction (125.6 g). This fraction was separated on an MCI-gel column (MeOH−H_2O from 8:2 to 10:0) to obtain six fractions (Fr. A−F). Fr. A (18.5 g) was chromatographed on a silica gel column, eluted with petroleum ether−acetone (from 50:1 to 10:1), to yield three fractions (Fr. A1−A3). Fr. A1 (8.3 g) was further purified by preparative HPLC (MeOH−H_2O, 98:2) to afford **3** (4.8 g) and **4** (1.1 g). In the same way, **5** (120 mg) and **7** (86 mg) were obtained from Fr. A2 (2.5 g). Fr. B (14.9 g) was subjected to silica gel column chromatography, eluted with petroleum ether−EtOAc (from 20:1 to 10:1), to yield Fr. B1−B3. On further purification by preparative HPLC (MeOH−H_2O, 95:5), Fr. B1 (3.5 g) afforded **1** (3 mg) and **2** (2 mg). Fr. B2 (850 mg) was separated by semipreparative HPLC (MeCN−H_2O, 92:8) to afford **6** (3 mg) and **11** (86 mg). Using preparative TLC (petroleum ether−acetone and petroleum ether−EtOAc), combined with semipreparative HPLC with different solvent systems (MeOH−H_2O and MeCN−H_2O), Fr. C (7.4 g) afforded compounds **8** (26 mg), **9** (8 mg), **10** (5 mg), **12** (130 mg), **13** (38 mg), **23** (58 mg), **24** (35 mg), **25** (30 mg), and **39** (24 mg). Similarly, compounds **14** (1.0 g), **15** (430 mg), **16** (260 mg), **31** (8 mg), **32** (12 mg), **33** (6 mg), **34** (11 mg), **37** (29 mg), **38** (32 mg), and **40** (32 mg) were obtained from Fr. D (16.8 g), compounds **17** (42 mg), **18** (14 mg), **19** (1.7 g), **20** (130 mg), **26** (140 mg), **27** (104 mg), **35** (28 mg), and **36** (15 mg) were from Fr. E (19.3 g), and compounds **21** (540 mg), **22** (140 mg), **28** (37 mg), **29** (14 mg), and **30** (46 mg) were from Fr. F (13.4 g).

Hyphenrone G (4): colorless gum; $[\alpha]^{26}_D$ +26 (*c* 0.4, MeOH); UV (MeOH) λ_{max} (log ε) 204 (4.13) nm; IR (KBr) ν_{max} 3441, 2967, 2926, 2856, 1776, 1741, 1676, 1450, 1378, 1238, 1117 cm^{-1}; ^{1}H and ^{13}C NMR data, see Table 1; FABMS *m*/*z* 565 $[M - H]^-$; HRTOFMS *m*/*z* 589.3871 $[M + Na]^+$ (calcd for $C_{36}H_{54}O_5Na$, 589.3868).

Hyphenrone H (7): colorless gum; $[\alpha]^{20}_D$ −4 (*c* 0.1, MeOH); UV (MeOH) λ_{max} (log ε) 203 (4.12) nm; IR (KBr) ν_{max} 2969, 2926, 2856,

DOI: 10.1021/acs.jnatprod.5b00057
J. Nat. Prod. 2015, 78, 885−895

Scheme 5. Proposed Biosynthetic Pathway of Group III PPAPs: Direct Cyclization of MPAPs Generating Four Different Carbon Scaffolds, Involving 17 and 18 with a Novel Carbon Skeleton

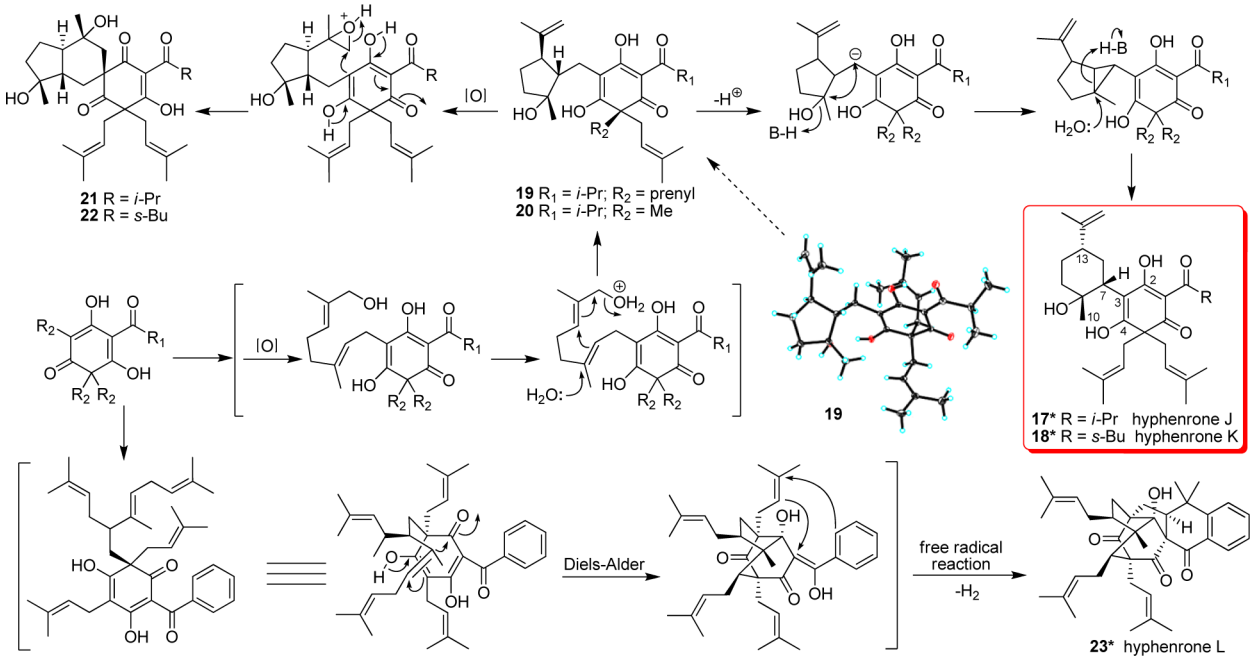

1813, 1759, 1736, 1711, 1629, 1452, 1380, 1125, 1034, 845, 785 cm^{-1}; ^1H and ^{13}C NMR data, see Table 1; ESIMS *m/z* 589 $[M + Na]^+$; HRTOFMS *m/z* 589.3857 $[M + Na]^+$ (calcd for $C_{36}H_{54}O_5Na$, 589.3868).

*Hyphenrone I (**9**):* white powder; $[\alpha]^{21}_D$ +22 (*c* 0.1, MeOH); UV (MeOH) λ_{max} (log ε) 205 (4.10), 254 (4.02) nm; IR (KBr) ν_{max} 2967, 2930, 1810, 1756, 1724, 1665, 1453, 1385, 1111, 1036 cm^{-1}; ^1H and ^{13}C NMR data, see Table 1; ESIMS *m/z* 545 $[M + Na]^+$; HRTOFMS *m/z* 545.3242 $[M + Na]^+$ (calcd for $C_{33}H_{46}O_5Na$, 545.3242).

*Hyphenrone J (**17**):* light yellow gum; $[\alpha]^{23}_D$ −49 (*c* 0.2, MeOH); UV (MeOH) λ_{max} (log ε) 206 (4.00), 224 (3.98), 356 (3.88) nm; IR (KBr) ν_{max} 3419, 2965, 2928, 2859, 1727, 1637, 1585, 1519, 1439, 1377, 1311, 1261, 1092,1030, 803 cm^{-1}; ^1H and ^{13}C NMR data, see Table 4; ESIMS *m/z* 507 $[M + Na]^+$; HRTOFMS *m/z* 507.3093 $[M + Na]^+$ (calcd for $C_{30}H_{44}O_5Na$, 507.3086).

*Hyphenrone K (**18**):* light yellow gum; $[\alpha]^{23}_D$ +66 (*c* 0.1, MeOH); UV (MeOH) λ_{max} (log ε) 207 (4.09), 225 (4.04), 349 (3.91) nm; IR (KBr) ν_{max} 3421, 2965, 2930, 2874, 1730,1636, 1585, 1520, 1456, 1377, 1311, 1261, 1117,1079, 802 cm^{-1}; ^1H and ^{13}C NMR data, see Table 4; ESIMS *m/z* 521 $[M + Na]^+$; HRTOFMS *m/z* 499.3429 $[M + H]^+$ (calcd for $C_{31}H_{47}O_5$, 499.3423).

*Hyphenrone L (**23**):* light yellow gum; $[\alpha]^{23}_D$ −12 (*c* 0.1, MeOH); UV (MeOH) λ_{max} (log ε) 206 (4.31), 253 (3.98) nm; IR (KBr) ν_{max} 3439, 2966, 2925, 1736, 1708, 1668, 1630, 1601, 1451, 1378, 1328, 1260, 1117, 761 cm^{-1}; ^1H and ^{13}C NMR data, see Table 5; TOFMS *m/z* 591 $[M + Na]^+$; HRTOFMS *m/z* 591.3444 $[M + Na]^+$ (calcd for $C_{38}H_{48}O_4Na$, 591.3450).

*Hyphenrone M (**29**):* colorless gum; $[\alpha]^{20}_D$ −82 (*c* 0.2, MeOH); UV (MeOH) λ_{max} (log ε) 202 (4.24), 245 (3.91) nm; IR (KBr) ν_{max} 3432, 2972, 2929, 1721, 1690, 1629, 1448, 1389, 1245, 1155, 1020 cm^{-1}; ^1H and ^{13}C NMR data, see Tables 2 and 3; ESIMS *m/z* 557 $[M + Na]^+$; HREIMS *m/z* 534.2962 $[M]^+$ (calcd for $C_{33}H_{42}O_6$, 534.2981).

*Hyphenrone N (**30**):* light yellow gum; $[\alpha]^{23}_D$ −89 (*c* 0.2, MeOH); UV (MeOH) λ_{max} (log ε) 205 (4.15), 246 (3.85) nm; IR (KBr) ν_{max} 3433, 2969, 2927, 2876, 1722, 1690, 1448, 1389, 1250, 1154, 1106, 693 cm^{-1}; ^1H and ^{13}C NMR data, see Tables 2 and 3; ESIMS *m/z* 625 $[M + Na]^+$; HREIMS *m/z* 602.3613 $[M]^+$ (calcd for $C_{38}H_{50}O_6$, 602.3607).

*Hyphenrone O (**32**):* colorless gum; $[\alpha]^{23}_D$ −9 (*c* 0.1, MeOH); UV (MeOH) λ_{max} (log ε) 205 (4.30), 245 (3.99) nm; IR (KBr) ν_{max} 2970, 2928, 1737, 1700, 1629, 1449, 1384, 1237, 1122, 1062, 689 cm^{-1}; ^1H and ^{13}C NMR data, see Tables 2 and 3; ESIMS *m/z* 607 $[M + Na]^+$; HREIMS *m/z* 584.3499 $[M]^+$ (calcd for $C_{38}H_{48}O_5$, 584.3502).

*Hyphenrone P (**33**):* colorless gum; $[\alpha]^{22}_D$ −83 (*c* 0.1, MeOH); UV (MeOH) λ_{max} (log ε) 204 (4.51), 245 (4.26) nm; IR (KBr) ν_{max} 2961, 2929, 2872, 1736, 1703, 1686, 1448, 1390, 1370, 1238, 1124, 688 cm^{-1}; ^1H and ^{13}C NMR data, see Tables 2 and 3; ESIMS *m/z* 525 $[M + Na]^+$; HREIMS *m/z* 502.3077 $[M]^+$ (calcd for $C_{33}H_{42}O_4$, 502.3083).

*Hyphenrone Q (**34**):* colorless gum; $[\alpha]^{22}_D$ −4 (*c* 0.2, MeOH); UV (MeOH) λ_{max} (log ε) 204 (4.25), 246 (4.03) nm; IR (KBr) ν_{max} 2959, 2927, 2876, 1737, 1704, 1687, 1629, 1448, 1392, 1235, 1104 cm^{-1}; ^1H and ^{13}C NMR data, see Tables 2 and 3; ESIMS *m/z* 525 $[M + Na]^+$; HREIMS *m/z* 502.3092 $[M]^+$ (calcd for $C_{33}H_{42}O_4$, 502.3083).

Crystallographic Data of 11. $C_{34}H_{54}O_4$, M = 526.77, orthorhombic, a = 9.3781(2) Å, b = 12.6568(3) Å, c = 27.0482(6) Å, $\alpha = \beta = \gamma$ = 90°, V = 3210.53(12) $Å^3$, T = 100(2) K, space group $P2_12_12_1$, Z = 4, μ(Cu Kα) = 0.537 mm^{-1}, 12 272 reflections measured, 4892 independent reflections (R_{int} = 0.0366). The final R_1 values were 0.0794 ($I > 2\sigma(I)$). The final $wR(F^2)$ values were 0.2097 ($I > 2\sigma(I)$). The final R_1 values were 0.0798 (all data). The final $wR(F^2)$ values were 0.2106 (all data). The goodness of fit on F^2 was 1.186. Flack parameter = 0.2(3). The Hooft parameter is 0.11(7) for 1815 Bijvoet pairs. Crystallographic data for **11** have been deposited at the Cambridge Crystallographic Data Center (deposition number CCDC 962625). Copies of the data can be obtained free of charge via www.ccdc.cam.ac.uk.

Crystallographic Data of 13. $C_{36}H_{54}O_5$, M = 566.79, monoclinic, a = 9.3216(4) Å, b = 13.2025(6) Å, c = 13.8291(6) Å, $\alpha = \gamma$ = 90°, β = 107.9680(10)°, V = 1618.92(12) $Å^3$, T = 100(2) K, space group $P2_1$, Z = 2, μ(Cu Kα) = 0.592 mm^{-1}, 19 174 reflections measured, 5414 independent reflections (R_{int} = 0.0463). The final R_1 values were 0.0678 ($I > 2\sigma(I)$). The final $wR(F^2)$ values were 0.1822 ($I > 2\sigma(I)$). The final R_1 values were 0.0679 (all data). The final $wR(F^2)$ values were 0.1827 (all data). The goodness of fit on F^2 was 1.079. Flack parameter = 0.09(19). The Hooft parameter is 0.11(5) for 2319 Bijvoet pairs (CCDC 962624).

Crystallographic Data of 19. $C_{30}H_{44}O_5$, M = 484.65, orthorhombic, a = 10.0575(3) Å, b = 16.0634(4) Å, c = 17.3900(4) Å, $\alpha = \beta = \gamma$ = 90°, V = 2809.49(13) $Å^3$, T = 100(2) K, space group $P2_12_12_1$, Z = 4, μ(Cu Kα) = 0.604 mm^{-1}, 16 676 reflections measured,

DOI: 10.1021/acs.jnatprod.5b00057
J. Nat. Prod. 2015, 78, 885−895

Table 4. ^{13}C (150 MHz) and ^{1}H (600 MHz) NMR Spectroscopic Data of 17 and 18

	17[a]		18[a]	
no.	δ_C, type	δ_H mult. (J in Hz)	δ_C, type	δ_H mult. (J in Hz)
1	107.4, C		108.0, C	
2	191.1, C		190.6, C	
3	112.6, C		112.5, C	
4	177.9, C		179.0, C	
5	58.5, C		58.7, C	
6	196.4, C		196.7, C	
7	42.2, CH	3.28 dd (13.2, 3.8)	42.2, CH	3.28 dd (13.2, 3.8)
8	31.8, CH_2	α 1.96 m	31.8, CH_2	α 1.98 m
		β 1.29 m		β 1.28 m
9	73.7, C		73.5, C	
10	27.9, CH_3	1.23 s	28.0, CH_3	1.22 s
11	40.4, CH_2	α 1.90 m	40.5, CH_2	α 1.86 m
		β 1.69 m		β 1.66 m
12	27.3, CH_2	α 1.79 m	27.4, CH_2	α 1.80 m
		β 1.61 m		β 1.60 m
13	46.4, CH	2.11 m	46.5, CH	2.10 m
C-14	150.6, C		150.7, C	
C-15	108.9, CH_2	4.71 s	108.8, CH_2	4.71 s
		4.69 s		4.68 s
16	21.1, CH_3	1.73 s	21.1, CH_3	1.73 s
17	206.4, C		205.8, C	
18	35.6, CH	4.10 sept (6.8)	42.1, CH	4.00 m (6.8)
19	19.2, CH_3	1.08 d (6.8)	17.2, CH_3	1.08 d (6.8)
20	19.3, CH_3	1.09 d (6.8)	27.3, CH_2	1.70 m
				1.35 m
21			12.3, CH_3	0.87 t (6.8)
22	39.0, CH_2	2.58 m	39.5, CH_2	2.56 m
23	119.7, CH	4.80 t (7.9)	119.9, CH	4.81 t (7.9)
24	134.3, C		134.1, C	
25	26.0, CH_3	1.50 s	26.0, CH_3	1.51 s
26	18.0, CH_3	1.55 s	18.0, CH_3	1.56 s
27	39.3, CH_2	2.59 overlap	38.8, CH_2	2.58 overlap
28	120.0, CH	4.86 t (7.5)	120.1, CH	4.86 t (7.6)
29	134.4, C		134.2, C	
30	26.1, CH_3	1.52 s	26.1, CH_3	1.50 s
31	18.0, CH_3	1.56 s	18.0, CH_3	1.55 s

[a]Recorded in acetone-d_6.

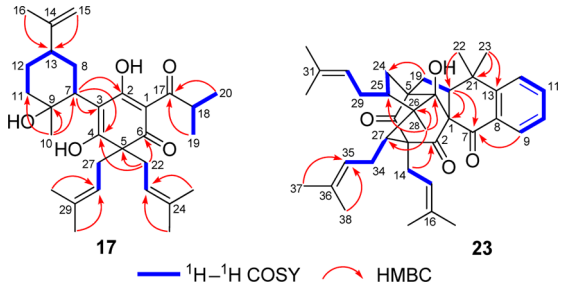

Figure 3. Key HMBC and $^{1}H-^{1}H$ COSY correlations of 17 and 23.

5061 independent reflections (R_{int} = 0.0345). The final R_1 values were 0.0345 ($I > 2\sigma(I)$). The final $wR(F^2)$ values were 0.0899 ($I > 2\sigma(I)$). The final R_1 values were 0.0346 (all data). The final $wR(F^2)$ values were 0.0901 (all data). The goodness of fit on F^2 was 1.087. Flack parameter = 0.04(13). The Hooft parameter is 0.07(4) for 2131 Bijvoet pairs (CCDC 963510).

Crystallographic Data of 26. $2(C_{33}H_{40}O_5)\cdot 3(CH_4O)$, M = 1129.43, monoclinic, a = 18.0066(3) Å, b = 13.5854(2) Å, c = 13.2739(2) Å, $\alpha = \gamma = 90°$, β = 93.8980(10)°, V = 3239.64(9) Å^3, T = 100(2) K, space group $C2$, Z = 2, μ(Cu Kα) = 0.631 mm^{-1}, 21 434 reflections measured, 5565 independent reflections (R_{int} = 0.0464). The final R_1 values were 0.0557 ($I > 2\sigma(I)$). The final $wR(F^2)$ values were 0.1602 ($I > 2\sigma(I)$). The final R_1 values were 0.0567 (all data). The final $wR(F^2)$ values were 0.1618 (all data). The goodness of fit on F^2 was 1.052. Flack parameter = 0.2(2). The Hooft parameter is 0.10(6) for 2577 Bijvoet pairs (CCDC 962622).

Table 5. ^{1}H (600 MHz) and ^{13}C (150 MHz) NMR Spectroscopic Data of 23[a]

no.	δ_C, type	δ_H mult. (J in Hz)	no.	δ_C, type	δ_H mult. (J in Hz)
1	71.1, C		21	38.4, C	
2	205.1, C		22	27.1, CH_3	1.34 s
3	69.9, C		23	30.2, CH_3	1.13 s
4	215.9, C		24	33.9, CH_2	β 1.54 m
5	71.5, C				α 1.88 dd (7.8,10.8)
6	91.6, C		25	61.2, CH	1.79 m
7	199.9, C		26	46.8, C	
8	137.4, C		27	54.8, CH	1.76 m
9	127.9, CH	7.69 d (7.5)	28	14.5, CH_3	1.43 s
10	127.6, CH	7.35 t (7.5)	29	33.4, CH_2	2.23 m
11	134.7, CH	7.56 t (7.5)			2.08 m
12	124.8, CH	7.43 d (7.5)	30	124.7, CH	5.03 m
13	152.2, C		31	132.9, C	
14	24.4, CH_2	2.44 dd (9.8, 15.5)	32	25.9, CH_3	1.68 s
		2.19 m	33	18.1, CH_3	1.62 s
15	120.5, CH	4.98 m	34	27.8, CH_2	2.17 m
16	134.8, C				1.60 m
17	26.2, CH_3	1.66 s	35	126.9, CH	4.90 m
18	17.9, CH_3	1.57 s	36	132.3, C	
19	29.6, CH_2	β 2.15 m	37	26.0, CH_3	1.67 s
		α 1.93 dd (8.8,12.0)	38	18.4, CH_3	1.64 s
20	58.6, CH	2.60 t (8.8)			

[a]Recorded in methanol-d_4.

Table 6. Cytotoxicities of Selected PPAPs against Five Cancer Cell Lines (IC_{50} μM)

compound[a]	HL-60	SMMC-7721	A-549	MCF-7	SW480
5	18.6	>40	>40	>40	>40
9	19.8	30.1	24.6	>40	>40
10	12.2	25.5	16.0	24.1	>40
13	4.7	18.2	12.6	11.6	>40
17	1.7	3.5	3.0	4.9	7.0
19	2.3	7.4	5.9	7.2	8.9
23	14.0	20.8	19.3	27.7	>40
24	23.6	16.6	19.8	27.7	>40
26	16.5	16.5	14.2	14.1	17.4
27	14.5	14.2	13.3	17.6	19.1
28	17.1	20.8	24.9	28.4	>40
30	14.5	11.8	13.9	14.4	16.0
DDP[b]	1.1	6.8	6.0	15.4	16.3
Taxol[b]	<0.008	<0.008	<0.008	<0.008	<0.008

[a]Other isolates with IC_{50} > 40 μM for all cell lines are not listed. [b]*cis*-Platin and taxol were used as positive controls.

Crystallographic Data of 38. $C_{30}H_{36}O_4$, M = 460.59, monoclinic, a = 10.75090(10) Å, b = 7.76550(10) Å, c = 14.8907(2) Å, $\alpha = \gamma = 90°$, β = 99.69°, V = 1225.44(3) Å^3, T = 100(2) K, space group $P2_1$, Z = 2, μ(Cu Kα) = 0.642 mm^{-1}, 15 304 reflections measured, 4218 independent reflections (R_{int} = 0.0261). The final R_1 values were

DOI: 10.1021/acs.jnatprod.5b00057
J. Nat. Prod. 2015, 78, 885−895

0.0296 ($I > 2\sigma(I)$). The final $wR(F^2)$ values were 0.0786 ($I > 2\sigma(I)$). The final R_1 values were 0.0297 (all data). The final $wR(F^2)$ values were 0.0787 (all data). The goodness of fit on F^2 was 1.030. Flack parameter = 0.01(13). The Hooft parameter is 0.01(3) for 1773 Bijvoet pairs (CCDC 962623).

General Procedure for the Retro-Aldol Reaction of 3. To a solution of **3** (0.1 mmol, 1.0 equiv) in MeCN (0.5 mL) were added H_2O (0.2 mmol, 2.0 equiv) and piperidine (0.03 mmol, 0.3 equiv). The mixture was stirred at room temperature for 12 h under argon, after which it was filtered through a short pad of $MgSO_4$ and washed with dry CH_2Cl_2. The solvent was removed under vacuum, and the residue was chromatographed on silica gel (ether−EtOAc, 30:1) to give **5** (22.3 mg, 40%) as a colorless oil.

General Procedure for the Synthesis of 11. A mixture of **5** (10 mg, 0.018 mmol), MeOH (0.5 mL), and triethylamine (0.05 mL) was stirred at 50 °C for 24 h. The volatiles were removed under vacuum, and the residue was purified by flash silica gel column chromatography (ether−EtOAc, 15:1) to afford **11** as colorless crystals (3.7 mg, 39%).

Acetylcholinesterase Inhibitory Assay. The acetylcholinesterase (AChE) inhibitory activity of the compounds was assayed by the spectrophotometric method developed by Ellman et al.[21] with slight modifications. *S*-Acetylthiocholine iodide, *S*-butyrylthiocholine iodide, 5,5′-dithiobis(2-nitrobenzoic) acid (DTNB, Ellman's reagent), and acetylcholinesterase derived from human erythrocytes were purchased from Sigma Chemical. Compounds were dissolved in DMSO. The mixture containing 110 μL of phosphate buffer (pH 8.0), 10 μL of test compound (50 μM), and 40 μL of acetylcholinesterase (0.04 U/100 μL) was incubated for 20 min (30 °C). The reaction was initiated by the addition of 20 μL of DTNB (6.25 mM) and 20 μL of acetylthiocholine for AChE inhibitory activity, respectively. The hydrolysis of acetylthiocholine was monitored at 405 nm after 30 min. Tacrine was used as a positive control. All the reactions were performed in triplicate. The percentage inhibition was calculated as follows: % inhibition = $(E - S)/E \times 100$ (E is the activity of the enzyme without test compound and S is the activity of enzyme with test compound). Sample limitations precluded the testing of compounds **6** and **18**.

Cytotoxicity Bioassays. Colorimetric assays were performed to evaluate compound activity. The following human tumor cell lines were used: HL-60 human myeloid leukemia, SMMC-7721 human hepatocarcinoma, A-549 lung cancer, MCF-7 breast cancer, and SW-480 human pancreatic carcinoma. All cells were cultured in RPMI-1640 or DMEM medium (Hyclone, Logan, UT, USA), supplemented with 10% fetal bovine serum (Hyclone) at 37 °C in a humidified atmosphere with 5% CO_2. Cell viability was assessed by conducting colorimetric measurements of the amount of insoluble formazan formed in living cells based on the reduction of 3-(4,5-dimethylthiazol-2-yl)-2,5-diphenyltetrazolium bromide (MTT). Briefly, 100 μL of adherent cells were seeded into each well of a 96-well cell culture plate and allowed to adhere for 12 h before test compound addition, while suspended cells were seeded just before this step, both with an initial density of 1×10^5 cells/mL in 100 μL of medium. Each tumor cell line was exposed to the test compound at various concentrations in triplicate for 48 h, with *cis*-platin (Sigma) as positive control. After the incubation, MTT (100 μg) was added to each well, and the incubation continued for 4 h at 37 °C. The cells were lysed with 100 μL of 20% SDS−50% DMF after removal of 100 μL of medium. The optical density of the lysate was measured at 595 nm in a 96-well microtiter plate reader (Bio-Rad 680). The IC_{50} value of each compound was calculated by Reed and Muench's method.

■ ASSOCIATED CONTENT

Ⓢ Supporting Information

The original MS, ^1H and ^{13}C NMR, HSQC, $^1H-^1H$ COSY, HMBC, and ROESY NMR spectra for all the new compounds and crystallographic files for **11**, **13**, **19**, **26**, and **38** in CIF format. This material is available free of charge via the Internet at http://pubs.acs.org.

■ AUTHOR INFORMATION

Corresponding Authors

*Tel and Fax: +86-871-65217971. E-mail: xugang008@mail.kib.ac.cn (G. Xu).

*E-mail: qinhongbo@mail.kib.ac.cn (H. B. Qin).

Author Contributions

‖X. W. Yang and M. M. Li contributed equally.

Notes

The authors declare no competing financial interest.

■ ACKNOWLEDGMENTS

The work was supported financially by the National Natural Sciences Foundation of China (20972167), the Young Academic Leader Raising Foundation of Yunnan Province (No. 2009CI073), the National Science and Technology Support Program of China (2013BAI11B02), the foundation from Chinese Academy of Sciences to G.X., and the Program of "One Hundred Talented People" to H.B.Q.

■ REFERENCES

(1) Ciochina, R.; Grossman, R. B. *Chem. Rev.* **2006**, *106*, 3963−3986.

(2) (a) Singh, I. P.; Bharate, S. B. *Nat. Prod. Rep.* **2006**, *23*, 558−591. (b) Zhang, Q.; Mitasev, B.; Qi, J.; Porco, J. A., Jr. *J. Am. Chem. Soc.* **2010**, *132*, 14212−14215. (c) Qi, J.; Beeler, A. B.; Zhang, Q.; Porco, J. A., Jr. *J. Am. Chem. Soc.* **2010**, *132*, 13642−13644. (d) Shimizu, Y.; Shi, S.-L.; Usuda, H.; Kanai, M.; Shibasaki, M. *Angew. Chem., Int. Ed.* **2010**, *49*, 1103−1106. (e) Biber, N.; Mows, K.; Plietker, B. *Nat. Chem.* **2011**, *3*, 938−942. (f) Richard, J.-A.; Pouwer, R. H.; Chen, D. Y.-K. *Angew. Chem., Int. Ed.* **2012**, *51*, 4536−4561. (g) Sparling, B. A.; Moebius, D. C.; Shair, M. D. *J. Am. Chem. Soc.* **2013**, *135*, 644−647. (h) Tian, W. J.; Yu, Y.; Yao, X. J.; Chen, H. F.; Dai, Y.; Zhang, X. K.; Yao, X. S. *Org. Lett.* **2014**, *16*, 3448−3451. (i) Grenning, A. J.; Boyce, J. H.; Porco, J. A., Jr. *J. Am. Chem. Soc.* **2014**, *136*, 11799−11804.

(3) (a) Adam, P.; Arigoni, D.; Bacher, A.; Eisenreich, W. *J. Med. Chem.* **2002**, *45*, 4786−4793. (b) Boubakir, Z.; Beuerle, T.; Liu, B.; Beerhues, L. *Phytochemistry* **2005**, *66*, 51−57. (c) Karppinen, K.; Hokkanen, J.; Tolonen, A.; Mattila, S.; Hohtola, A. *Phytochemistry* **2007**, *68*, 1038−1045. (d) Nualkaew, N.; Morita, H.; Shimokawa, Y.; Kinjo, K.; Kushiro, T.; De-Eknamkul, W.; Ebizuka, Y.; Abe, I. *Phytochemistry* **2012**, *77*, 60−69.

(4) Maisenbacher, P.; Kovar, K. A. *Planta Med.* **1992**, *58*, 291−293.

(5) Henry, G. E.; Jacobs, H.; Carrington, C. M. S.; McLean, S.; Reynolds, W. F. *Tetrahedron Lett.* **1996**, *37*, 8663−8666.

(6) Avato, P. In *Studies in Natural Products Chemistry*; Atta-ur Rahman, Ed.; Elsevier: Amsterdanm, 2005; Vol. *30*, pp 603−634.

(7) Griffith, T. N.; Varela-Nallar, L.; Dinamarca, M. C.; Inestrosa, N. C. *Curr. Med. Chem.* **2010**, *17*, 391−406.

(8) (a) Yang, X. W.; Deng, X.; Liu, X.; Wu, C. Y.; Li, X. N.; Wu, B.; Luo, H. R.; Li, Y.; Xu, H. X.; Zhao, Q. S.; Xu, G. *Chem. Commun.* **2012**, *48*, 5998−6000. (b) Liu, X.; Yang, X. W.; Chen, C. Q.; Wu, C. Y.; Zhang, J. J.; Ma, J. Z.; Wang, H.; Yang, L. X.; Xu, G. *J. Nat. Prod.* **2013**, *76*, 1612−1618. (c) Yang, X. W.; Ding, Y.; Zhang, J. J.; Liu, X.; Yang, L. X.; Li, X. N.; Ferreira, D.; Walker, L. A.; Xu, G. *Org. Lett.* **2014**, *16*, 2434−2437. (d) Zhang, J. J.; Yang, J.; Liao, Y.; Yang, X. W.; Ma, J. Z.; Xiao, Q. L.; Yang, L. X.; Xu, G. *Org. Lett.* **2014**, *16*, 4912−4915.

(9) Lan, M. In *South Yunnan Materia Medica*; Wu, Z. Y., Gao, L., Ed.; Science Press: Kunming, 2008; Vol. *1*, pp 236−240.

(10) (a) Wu, Q. L.; Wang, S. P.; Du, L. J.; Yang, J. S.; Xiao, P. G. *Phytochemistry* **1998**, *49*, 1395−1402. (b) Chen, X. Q.; Li, Y.; Cheng, X.; Wang, K.; He, J.; Pan, Z. H.; Li, M. M.; Peng, L. Y.; Xu, G.; Zhao, Q. S. *Chem. Biodiversity* **2010**, *7*, 196−204. (c) Guo, N.; Chen, X. Q.; Zhao, Q. S. *Acta Bot. Yunnan.* **2008**, *30*, 515−518.

(11) (a) Wu, J.; Cheng, X. F.; Harrison, L. J.; Goh, S.-H.; Sim, K.-Y. *Tetrahedron Lett.* **2004**, *45*, 9657−9659. (b) Nicolaou, K. C.; Carenzi, G. E. A.; Jeso, V. *Angew. Chem., Int. Ed.* **2005**, *44*, 3895−3899.

DOI: 10.1021/acs.jnatprod.5b00057
J. Nat. Prod. 2015, 78, 885−895

(12) Verotta, L.; Appendino, G.; Jakupovic, J.; Bombardelli, E. *J. Nat. Prod.* **2000**, *63*, 412−415.
(13) (a) Verotta, L.; Appendino, G.; Belloro, E.; Jakupovic, J.; Bombardelli, E. *J. Nat. Prod.* **1999**, *62*, 770−772. (b) Vugdelija, S.; Vajs, V.; Trifunovic, S.; Djokovic, D.; Milosavljevic, S. *Molecules* **2000**, *5*, M158.
(14) (a) Schwerfeger, H.; Fokin, A. A.; Schreiner, P. R. *Angew. Chem., Int. Ed.* **2008**, *47*, 1022−1036. (b) Van der Schyf, C. J.; Geldenhuys, W. J. *Neurotherapeutics* **2009**, *6*, 175−186. (c) Wanka, L.; Iqbal, K.; Schreiner, P. R. *Chem. Rev.* **2013**, *113*, 3516−3604.
(15) Liu, J.; Obando, D.; Liao, V.; Lifa, T.; Codd, R. *Eur. J. Med. Chem.* **2011**, *46*, 1949−1963.
(16) (a) Hu, L. H.; Sim, K. Y. *Tetrahedron Lett.* **1998**, *39*, 7999−8002. (b) Hu, L. H.; Sim, K. Y. *Org. Lett.* **1999**, *1*, 879−882. (c) Hu, L. H.; Sim, K. Y. *Tetrahedron Lett.* **1999**, *40*, 759−762. (d) Ishida, Y.; Shirota, O.; Sekita, S.; Someya, K.; Tokita, F.; Nakane, T.; Kuroyanagi, M. *Chem. Pharm. Bull.* **2010**, *58*, 336−343. (e) Zeng, Y. H.; Osman, K.; Xiao, Z. Y.; Gibbons, S.; Mu, Q. *Phytochem. Lett.* **2012**, *5*, 200−205. (f) Liu, X.; Yang, X. W.; Chen, C. Q.; Wu, C. Y.; Zhang, J. J.; Ma, J. Z.; Wang, H.; Zhao, Q. S.; Yang, L. X.; Xu, G. *Nat. Prod. Bioprospect.* **2013**, *3*, 233−237. (g) Tian, W. J.; Qiu, Y. Q.; Jin, X. J.; Chen, H. F.; Yao, X. J.; Dai, Y.; Yao, X. S. *Tetrahedron* **2014**, *70*, 7912−7916. (h) Zhu, H.; Chen, C.; Yang, J.; Li, X. N.; Liu, J.; Sun, B.; Huang, S. X.; Li, D.; Yao, G.; Luo, Z.; Li, Y.; Zhang, J.; Xue, Y.; Zhang, Y. *Org. Lett.* **2014**, *16*, 6322−6325.
(17) Lin, Y. L.; Wu, Y. S. *Helv. Chim. Acta* **2003**, *86*, 2156−2163.
(18) (a) Flack, H. D. *Acta Crystallogr.* **1983**, *A39*, 876−881. (b) Hooft, R. W. W.; Straver, L. H.; Spek, A. L. *J. Appl. Crystallogr.* **2008**, *4*, 96−103.
(19) (a) Decosterd, L. A.; Stoeckli-Evans, H.; Chapuis, J.-C.; Sordat, B.; Hostettmann, K. *Helv. Chim. Acta* **1989**, *72*, 1833−1845. (b) Hashida, W.; Tanaka, N.; Kashiwada, Y.; Sekiya, M.; Ikeshiro, Y.; Takaishi, Y. *Phytochemistry* **2008**, *69*, 2225−2230.
(20) (a) Thoison, O.; Cuong, D. D.; Gramain, A.; Chiaroni, A.; Hung, N. V.; Sevenet, T. *Tetrahedron* **2005**, *61*, 8529−8535. (b) Pepper, H. P.; Lam, H. C.; Bloch, W. M.; George, J. H. *Org. Lett.* **2012**, *14*, 5162−5164. (c) Cholpisut, T.; Wong, P.; Thunwadee, R.; Sarot, C.; Uma, P.; Suwanna, D.; Surat, L. *J. Nat. Prod.* **2012**, *75*, 1660−1664.
(21) Alley, M. C.; Scudiero, D. A.; Monks, A.; Hursey, M. L.; Czerwinski, M. J.; Fine, D. L.; Abbott, B. J.; Mayo, J. G.; Shoemaker, R. H.; Boyd, M. R. *Cancer Res.* **1988**, *48*, 589−601.
(22) Ellman, G. L.; Courtney, K. D.; Andres, V., Jr.; Featherstone, R. M. *Biochem. Pharmacol.* **1961**, *7*, 88−95.
(23) (a) Yazaki, K.; Sasaki, K.; Tsurumaru, Y. *Phytochemistry* **2009**, *70*, 1739−1745. (b) Botta, B.; Menedez, P.; Zappia, G.; Alves de Lima, R.; Torge, R.; Delle Monache, G. *Curr. Med. Chem.* **2009**, *16*, 3414−3468. (c) Marin, M.; Manez, S. *Curr. Med. Chem.* **2013**, *20*, 272−279. (d) Bartmanska, A.; Tronina, T.; Poplonski, J.; Huszcza, E. *Curr. Drug Metab.* **2013**, *14*, 1083−1097.

DOI: 10.1021/acs.jnatprod.5b00057
J. Nat. Prod. 2015, 78, 885−895